Materials Today Bio 10 (2021) 100111

Contents lists available at ScienceDirect

Materials Today Bio

journal homepage: www.journals.elsevier.com/materials-today-bio

Dendrimer-based nanohybrids in cancer photomedicine

Zhijun Ouyang [a,c], Yue Gao [a,c], Mingwu Shen [a,**], Xiangyang Shi [a,b,*]

[a] State Key Laboratory for Modification of Chemical Fiber and Polymer Materials, Shanghai Engineering Research Center of Nano-Biomaterials and Regenerative Medicine, College of Chemistry, Chemical Engineering and Biotechnology, Donghua University, Shanghai, 201620, People's Republic of China
[b] CQM-Centro de Química da Madeira, Universidade da Madeira, 9020-105, Funchal, Portugal

ARTICLE INFO

Keywords:
Dendritic polymers
Hybrid nanoparticles
Phototherapy
Cancer theranostics

ABSTRACT

Cancer phototherapy with non-invasiveness and high therapeutical efficiency has emerged as a hot spot research in cancer management. Various nanomaterials have been involved in the development of novel photoactive agents to overcome the current limitations in cancer phototherapy. Dendrimers, as an excellent nanocarrier with unique physicochemical properties, have received extensive attention and much effort has been made in the development of dendrimer-based hybrid platforms for photomedicine applications. Dendrimers can be entrapped with photosensitive agents within their internal cavities and be surface modified with reactive molecules, constructing multifunctional nanoplatforms for cancer treatment. In this review, we concisely survey the design of several different kinds of dendrimer-based nanohybrids for cancer photomedicine applications, and provide an overview of their recent applications in molecular imaging, single-modality photothermal therapy or photodynamic therapy, combination therapy, and theranostics of cancer. In addition, we also briefly discuss the future perspectives in the area of dendrimer-based nanohybrids for cancer photomedicine.

1. Introduction

To improve the outcome of cancer treatment and relieve the pain of patients, physicians and scientists have long been exploring novel cancer treatment modalities with high selectivity and excellent therapeutical efficiency along with minimal invasiveness. Toward this end, cancer phototherapy, which exploits the light to trigger reaction against cancer, including photothermal therapy (PTT) and photodynamic therapy (PDT), has attracted widespread interest for precise targeting and efficient ablation of the irradiated cancer cells and tumor tissues [1–3]. However, the clinical translation of phototherapy is still limited by several factors such as superficial penetration depth of the laser, incomplete ablation outside the irradiation region, and possibilities of cancer recrudesce [4]. Thus, in the recent decades, tremendous efforts have turned to the versatile nanotechnology to construct multifunctional photomedicine nanoplatforms to overcome the current limitations in cancer phototherapy [5], realizing more personalized and long-lasting elimination of cancer, as well as facilitating cancer theranostics.

Dendrimers stand as a unique type of nanomaterials with potential applications in various biomedical fields. The term "dendrimer" originates from the Greek word of "dendrons", which has a three-dimensional branched structure [6–10]. The tree structure is composed of the initial core, repeating branching units initiated by the core, and terminal groups connected to the peripheric repeating branching units. Owing to their structural advantages, easy surface modifications, good stability, and biocompatibility, dendrimers have been extensively explored in drug/gene delivery [11–24], molecular imaging [25–31], nuclear medicine [32–37], and theranostics [28,38–44] of cancer. Recent advances show that dendrimer-based nanohybrids also hold great promise in cancer phototherapy to solve the current limitations of phototherapeutic reagents [45–49] with the structural advantages over other linear polymers such as easy surface modification with photoreactive agents along with other functional moieties (e.g., targeting ligands) and structural configuration with other components or nanoformulations *via* the hyperbranched units for enhanced tumor accumulation and penetration. In particular, the integration of inorganic and organic components with dendrimers could lead to improved stability and enhanced photothermal conversion efficiency of the nanohybrids, leading to their improved performances in imaging and therapeutical effects [50,51]. Herein, we concisely review the progresses in the design of dendrimer-based nanohybrids for

* Corresponding author.
** Corresponding author.
E-mail addresses: mwshen@dhu.edu.cn (M. Shen), xshi@dhu.edu.cn (X. Shi).
[c] These authors contributed equally to this work.

https://doi.org/10.1016/j.mtbio.2021.100111
Received 7 February 2021; Received in revised form 21 March 2021; Accepted 7 April 2021
Available online 16 April 2021

photomedicine applications, and provide an overview of their recent applications in molecular imaging, single-modality phototherapy (PDT and PTT), combination therapy, and theranostics of cancer (Scheme 1). The representative research progresses are listed in Table 1. We also clarify the possible blueprint for the development of multifunctional dendrimer-based hybrid cancer phototherapeutics.

2. Design of dendrimer-based hybrid photomedicine

2.1. Dendrimer-based metal and metal sulfide nanocomposites

Dendrimers can be used as templates or stabilizers to incorporate inorganic metal or metal sulfide nanoparticles (NPs) with strong surface plasmon resonance absorption and high photothermal conversion efficiency, such as gold (Au) NPs [52,53], Au nanorods (NRs) [54], Au nanoflowers (NFs) [55,56], Au nanostars (NSs) [57], and copper sulfide (CuS) NPs [58,59], controlling the size and stability of these inorganic NPs. As early as in 2007, Kono et al. [60] used poly (ethylene glycol) (PEG)-modified generation 4 (G4) poly (amidoamine) (PAMAM) dendrimers to entrap Au NPs *via* a facile $NaBH_4$ reduction chemistry, and found the thus formed dendrimer-entrapped Au NPs (Au DENPs) possessed light-induced heat generation ability. However, in this study, the simple morphology and small Au core size (2 nm) of Au DENPs lead to limited photothermal conversion efficiency, which is inadequate for further applications.

To improve the photothermal conversion efficiency, successive work by the same group of Kono [62] used PEG-cys-PAMAM dendrimers to grow Au NR core inside and synthesized Au NR-cored G2-G4 dendrimers, and discovered that the Au NR-cored G3 dendrimers owned the best stability with a favorable Au NR size around 31 nm. In addition, the same authors [63] made it feasible to increase the coverage of the dendrimers on the Au NR surface (0.28 per nm^2 Au NR) by conjugating PEG-PAMAM G4 with mercaptohexadecanoic acid–functionalized Au NRs. The created nanosystem could be further loaded with anticancer drug doxorubicin (DOX) for further biomedical applications. Different form the direct Au NR growth strategy, Cheng et al. [64] adopted a collision-regrowth method to synthesize dendrimer-stabilized Au NRs (Au DSNRs) *via* a shape transformation of Au DENPs during the dialysis process in the acidic buffer, resulting in the formation of Au NRs with a uniform size distribution (10 nm in diameter).

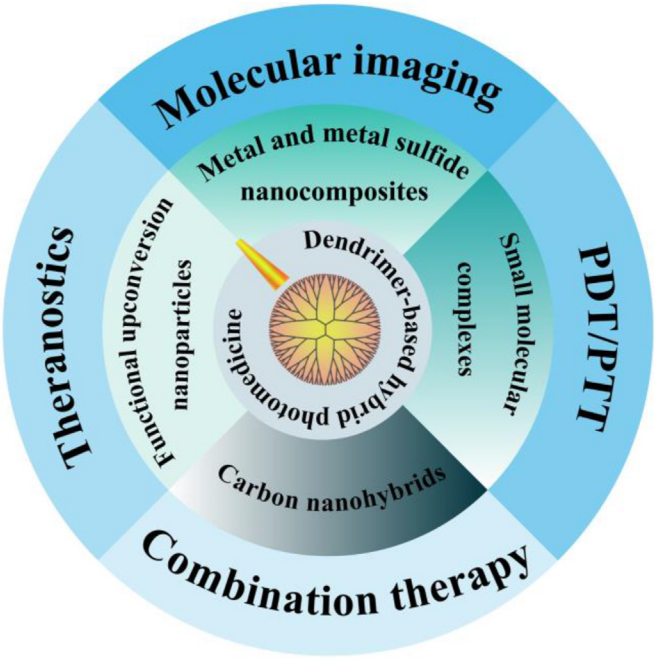

Scheme 1. The design and cancer theranostic applications of dendrimer-based hybrid photomedicine.

Besides Au NRs, Au NSs can also be combined with dendrimers. In a study by our group [48], we used the partially thiolated G3 PAMAM to assemble preformed Au NSs *via* Au–S bonding, and the formed dendrimer-assembled Au NSs could be further linked with arginine-glycine-aspartic (Arg-Gly-Asp, RGD) peptide, and displayed a high photothermal conversion efficiency (79%) and an ability to compact siRNA *via* electrostatic interaction through the dendrimer terminal amines. To integrate more functions within one nanoplatform, our group also prepared the dendrimer-stabilized Au NFs embedded with ultrasmall iron oxide (USIO) NPs [49]. In this work, the G5 PAMAM dendrimer-stabilized Au NPs (Au DSNPs) and citrate-stabilized USIO NPs were separately prepared, and the seed NPs composed of Au DSNPs and USIO NPs (Fe/Au molar ratio = 4:1) were produced by 1-(3-dimethylaminopropyl)-3-ethylcarbodiimide hydrochloride (EDC)-mediated covalent reaction to form Au NFs within an Au growth solution, and last the remaining terminal amines of PAMAM dendrimers were acetylated to neutralize the positive surface charge of the Au NFs. The formed Fe_3O_4/Au dendrimer-stabilized NFs (DSNFs) show improved photothermal conversion efficiency (82.7%) compared with the Fe-free Au DSNFs at the same Au concentration and display excellent photothermal stability.

In addition to Au, other types of metal or metal sulfide particles can also be incorporated with dendrimers. For instance, the Cheng group [50] used G5 PAMAM dendrimers as templates to entrap CuS, platinum (Pt), or palladium (Pd) NPs with a size smaller than 5 nm, modified *trans*-activating transcriptional activator or RGD peptide on the surface of dendrimers to enhance their cancer cell targeting and uptake, and decorated the dendrimers with a fluorescent probe for real-time tumor fluorescence imaging (Fig. 1A), which broaden the possibilities in dendrimer-based hybrid formulations. Our group [61] also reported the successful construction of dendrimer-entrapped CuS NPs by adopting a mild synthesis strategy *via* a reaction of $CuCl_2$ by Na_2S at a physiological temperature (37 °C) for 6 h. The G5 PAMAM dendrimers prefunctionalized with zwitterion of 1,3-propane (1,3-PS) and RGD peptide were used as templates. The formed multifunctional RGD-CuS DENPs were further complexed with pDNA through the leftover dendrimer surface amines (Fig. 1B) before biomedical applications. Owing to the fact that many types of 2-dimensional (2-D) inorganic materials have also been widely used for tumor phototherapy, our group [65] recently used the G5 PAMAM dendrimers partially functionalized with lipoic acid to assemble the hydrothermally synthesized MoS_2 nanoflakes *via* disulfide bond formation. The created G5-MoS_2 nanoflakes showed improved colloidal stability, size uniformity, and non-compromised heat generation ability. Meanwhile, due to the presence of dendrimer terminal amines, the formed G5-MoS_2 nanoflakes could be further complexed with siRNA for subsequent gene delivery applications.

2.2. Dendrimer-based small molecular complexes

Small molecular complexes have been used to conjugate with dendrimers to render them with photoactivities. For instance, Yuan et al. [66] reported a light-triggered size-switchable polymeric NP (denoted as SNPICG/Ce6). In brief, they modified indocyanine green (ICG) onto the surface of G3 PAMAM dendrimers to produce a photothermal agent (PAMAM-ICG) and then conjugated dendrimers with amphiphilic poly (ethylene glycol)-b-poly (ε-caprolactone) (PEG-b-PCL) copolymer through a singlet oxygen–responsive thioketal (TK) linker (PEG-b-PCL-TK) and PEG-b-PCL-COOH, respectively. Subsequently, the formed PEG-b-PCL-PAMAM-ICG and PEG-b-PCL-TK-PAMAM-ICG with a singlet oxygen–responsive TK linker were loaded with chlorin e6 (Ce6) to construct singlet oxygen–sensitive (SNPICG/Ce6) and insensitive (inSNPICG/Ce6) NPs. In another study [67], the authors used ICG to construct a pH-sensitive and charge-convertible nanocomplex based on graphene oxide (GO). In this work, they first used poly (L-lysine)

Table 1
Summary of the design of dendrimer-based hybrid photomedicine for biomedical applications.

Dendrimer-based hybrids	Functional components	Applications	Tumor types	Ref.
Metal and metal sulfide nanocomposites	G5 PAMAM dendrimer, Au NFs and Fe_3O_4	MR/PA/CT imaging, PTT/RT	4T1 tumors	[49]
	G3 PAMAM dendrimer, RGD, AuNSs and siRNA	CT imaging, PTT/Gene therapy	U87MG tumors	[48]
	G5 PAMAM dendrimer, CuS, Pt, or Pd	PTT	MDA-MB-231 tumors	[50]
	G5 PAMAM dendrimer, CuS, 1,3-PS, RGD and pDNA-HIC1	PA imaging, PTT/Gene therapy	MDA-MB-231 tumors	[61]
	G2-G4 PAMAM dendrimer, Au NRs	PTT	Colon carcinoma tumors	[62]
	G4 PAMAM dendrimer, Au NRs, PEG and DOX	PTT/Chemotherapy	Colon carcinoma tumors	[63]
	G5 PAMAM dendrimer, Au DSNRs	PTT	PC-9 tumors	[64]
	G5 PAMAM dendrimer, MoS_2 and siRNA	PTT/Gene therapy	4T1 tumors	[65]
Small molecular complexes	G3 PAMAM dendrimer, PEG, Ce6 and ICG	PTT/PDT	4T1 tumors	[66]
	G4 PAMAM dendrimer, GO, PLL and miR-21i	PTT/Gene therapy	MDA-MB-231 tumors	[67]
Carbon nanohybrids	G4 PPI dendrimer, Pc, LOGr and LHRH	Fluorescence imaging, PTT/PDT	A780/AD cells *in vitro*	[68]
Functional upconversion nanoparticles	G4 PAMAM dendrimer, UCNPs and Ce6	PDT	MCF-7 cells *in vitro*/4T1 tumors	[69]
	G5 PAMAM dendrimer, UCNPs, FA and DOX	Fluorescence imaging, light-triggered drug release	KB cells *in vitro*	[70]

Abbreviations: 1,3-PS, 1,3-propane sultone; Au DSNRs, dendrimer-stabilized gold nanorods; Au NFs, Au nanoflowers; Au NSs, Au nanostars; Ce6, chlorin e6; CT, computed tomography; CuS, copper sulfide; DOX, doxorubicin; FA, folate; G, generation, GO, graphene oxide; ICG, indocyanine green; LHRH, luteinizing hormone-releasing hormone; LOGr, low-oxygen graphene; miR-21i, anti-miR-21 oligonucleotide; MR, magnetic resonance; PA, photoacoustic; PAMAM, poly (amidoamine); Pc, phthalocyanine; Pd, palladium; pDNA-HIC1, plasmid DNA-encoding hypermethylation in cancer 1; PDT, photodynamic therapy; PEG, polyethylene glycol; PLL, poly (L-lysine); PPI, polypropylenimine; Pt, platinum; PTT, photothermal therapy; RGD, Arg-Gly-Asp; RT, radiation therapy; UCNPs, upconversion nanoparticles.

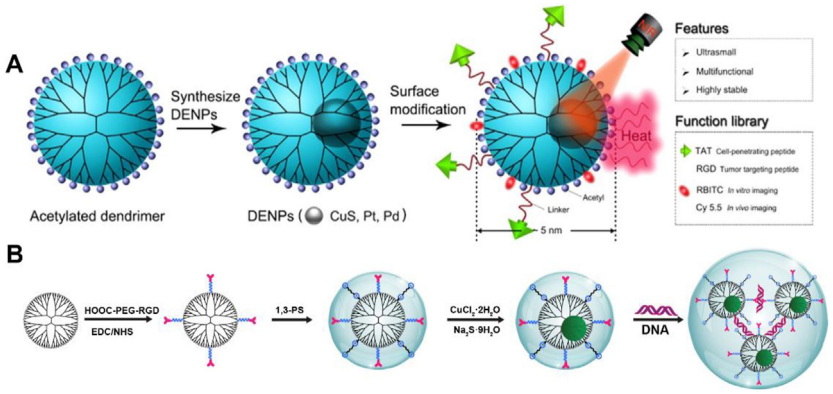

Fig. 1. (A) The synthesis of multifunctional dendrimer-entrapped inorganic NPs. Reproduced with permission [50], Copyright 2016, American Chemical Society. (B) The synthesis of RGD-CuS DENPs for pDNA loading. Reproduced with permission [61], Copyright 2021, American Chemical Society.

(PLL)-modified graphene (GP) to assemble citraconic to generate G-PLL-Cit (GPC) *via* EDC/N-hydroxysuccinimide (NHS) conjugation chemistry to have the charge-conversion ability, and then assembled the G4 PAMAM dendrimers on the surface of GPC to form GPCP. Finally, the GPCP was used to co-load ICG and microRNA-21 inhibitor (miR-21i) to obtain the GPCP/miR-21i/ICG nanocomplex for further biomedical applications (Fig. 2).

2.3. Dendrimer-based carbon nanohybrids

Carbon nanotubes (CNTs) [71–73] display unique structural and physical properties such as high absorption ability in near infrared (NIR) region compared with the well-known photothermal agents. Similarly, another carbon material, GP [74,75] has also been reported to have NIR light absorption. To fully take the advantages of dendrimer nanotechnology for photomedicine applications, these carbon-based materials have been connected to dendrimers to form nanohybrids. For instance, the Oki group [76] developed CNTs-PAMAM/G4-CdS photothermal agent consisting of G4 PAMAM covalently linked with CNTs and cadmium sulfide (CdS) NPs. In brief, the pristine CNTs were first carboxylated and acylated, and covalently grafted with G4 PAMAM dendrimer *via* iterative Michael addition by methyl methacrylate to the surface amino groups and amidation of terminal ester groups with ethylenediamine. Then CdS nanocrystals were deposited onto the surface of CNTs-G4 PAMAM hybrids by adding the cadmium acetate and Na_2S to react for 6 h to prepare the CNTs-G4 PAMAM-CdS. The formed CNTs-G4 PAMAM-CdS had a relatively higher photothermal conversion efficiency of 32% under a 980-nm NIR laser irradiation than some previously reported Au- or copper-based photothermal agents [77–79], presumably due to the coordination interaction between CNTs and CdS. Besides, the

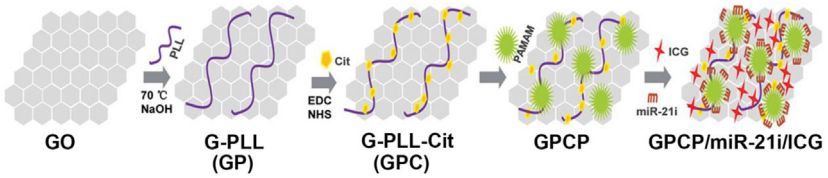

Fig. 2. Synthesis of GPCP/miR-21i/ICG through an assembly method. Reproduced with permission, Copyright 2020 [67], Wiley-VCH.

temperature could rapidly attain 64.1 °C after 7 min of laser irradiation. In another study, Taratula et al. [68] used polypropylenimine (PPI) dendrimers loaded with phthalocyanine (Pc) as a photosensitizer to covalently bind novel low-oxygen graphene (LOGr) nanosheets to form LOGr-Pc-PPIG4 nanohybrids with good water dispersibility. The LOGr-Pc-PPIG4 was further linked with PEG and luteinizing hormone-releasing hormone (LHRH) to enhance their biocompatibility and to be rendered with tumor targeting specificity, respectively. It should be noted that we categorize the type of dendrimer-based hybrids based on the major role of the component in the hybrids used for photomedicine. Hence, it is reasonable to see the different classifications of the hybrids with both small molecular agents and carbon materials co-existing.

2.4. Dendrimer-based functional upconversion NPs (UCNPs)

The lack of penetration of laser is an important issue to be addressed in promoting the development of cancer phototherapy. UCNPs have a unique anti-Stokes luminescence property because the 4f energy level of the lanthanides in the system endows them with deep-tissue penetration ability [80]. Chu and coworkers [69] recently constructed UCNPs with multiple carboxylate groups and coated them with amine-terminated G4 PAMAM dendrimers through electrostatic interaction in aqueous solution, followed by physical adsorption of Ce6. The hybrid UCNPs exhibit a polygonal morphology with a size of 16.0 ± 2.1 nm and α-phase crystallinity as confirmed by transmission electron microscopy and X-ray diffraction, respectively. In another study reported by Choi et al. [70], two types of silica-coated UCNPs (NaYF 4:Yb/Er or Yb/Tm) with different distinct emission wavelengths were first synthesized. The silica were aminated through salinization and partially modified with epoxy groups. Hence, photocaged doxorubicin (ONB-DOX) could be covalently linked onto the UCNP surface by reacting the amine groups of ONB-DOX with the surface epoxy groups of silica, and meanwhile, folate (FA)-modified G5 PAMAM dendrimers with carboxyl termini could be linked onto the UCNP surface *via* EDC coupling of the silica surface amines to generate UCN@(ONB-DOX) complexes, which enabled a UV light-mediated drug release (Fig. 3).

3. Biomedical applications of dendrimer-based photomedicine

3.1. Molecular imaging

Through the integration of optical properties of photo-active reagents and traits of other different components, dendrimer-based photomedicinal platforms can be applied as molecular imaging contrast agents

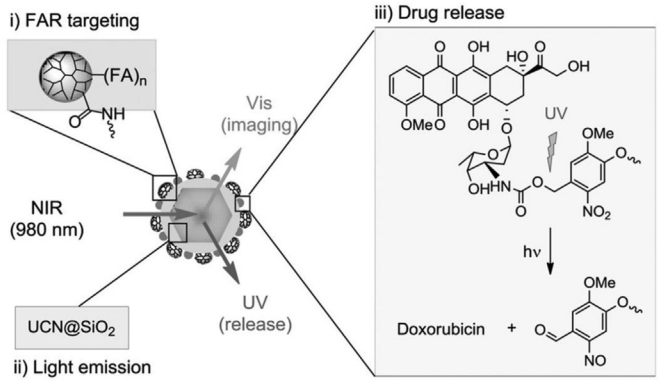

Fig. 3. Schematic overview of NIR-excited UCNPs covalently linked with multivalent FA-conjugated G5 PAMAM dendrimers for FA receptor-targeted cell imaging and UV light-mediated drug release. Reproduced with permission [70], Copyright 2015, Wiley-VCH.

to facilitate precision cancer diagnosis. In 2012, Andolina et al. [81] combined the utility of magnetic resonance (MR) and NIR fluorescence imaging agents within one dendrimer platform by incorporating Dy(III) and Yb(III) lanthanides with bimodal imaging properties within ester-amide dendrimers synthesized by Fréchet and colleagues [82] *via* chelating of different hexadentate-all-oxygen-donor ligands. The developed complexes could serve as a potential dual-mode NIR fluorescence/MR contrast agent with improved bioavailability, good water solubility, r_1 relaxivity of 7.60 mM/s due to the presence of Dy(III) chelated with TREN-bis(1-Me)-3,2-HOPOTAM-ethylamine), r_2 relaxivity of 23.8 mM/s due to the Yb(III) chelated with TREN-bis(1-Me)-3, 2-HOPOTAM-ethylamine-bisethylamine), and an NIR quantum yield of 0.17% evaluated in mouse serum. However, the imaging properties of these complexes are only preliminarily evaluated and no follow-up studies were performed.

In 2016, Li et al. [83] realized effective NIR imaging of early-stage esophageal squamous cell carcinoma model using a G5 PAMAM dendrimer labeled with an NIR dye Cy5.5 and conjugated with cyclic RGDfK peptide. In another study, Li and coworkers [84] were able to combine both MR and NIR fluorescence imaging using PEG-aptamer-modified G5 PAMAM dendrimers labeled with rhodamine, IR783 fluorophores and conjugated with paramagnetic Gd(III)-DTPA chelators on the dendrimer surface. The developed platform could be used for visualization of orthotopic liver tumor xenografts at an early stage through dual mode MR/fluorescence imaging. Similarly, Karki et al. constructed NIR fluorescent dye DL680- and DOTA-Gd(III) complex-conjugated G5 and G4 PAMAM dendrimers, respectively for dual-mode MR/fluorescence imaging of a mouse glioma model (U251 cells, a human glioma cell line) [85] and a mouse triple-negative breast cancer (TNBC, MDA-MB-231 cells, a human TNBC cell line) model [86], respectively.

3.2. PDT

Dendrimer-based nanohybrids have been applied for highly efficient PDT of tumors, overcoming the poor water-solubility and bioavailability of photosensitizers. For instance, Gao et al. [87] reported the use of the β-cyclodextrin (β-CD)-modified PAMAM dendrimers as a platform to co-deliver ICG and hematoporphyrin (HP) with NIR triggered-controllable photoactivities for PDT of cancer cells. The fluorescence of HP could be quenched by ICG, and could be recovered after ICG was degraded under an 808-nm laser irradiation. Cell apoptosis assay data revealed that cells treated with the formed dual-drug complexes had a high apoptosis rate of 97.6% under the 808/660 nm laser irradiation, while the cell apoptosis rate only achieved 6.42% and 8.78%, respectively, under the 660 nm and 880 nm laser irradiation, indicating that the developed co-delivery platform could effectively induce apoptosis of MCF-7 cells (a human breast cancer cell line) through PDT under the 808/660 nm laser irradiation. Unfortunately, this research did not go further to the *in vivo* stage.

Besides, organic/inorganic hybrid G4 PAMAM-UCNPs incorporated with Ce6 were also developed for PDT of cancer cells [69], and a better PDT efficiency *in vitro* with enhancement in cellular uptake of polycationic dendrimers was achieved under a 980-nm laser excitation than under a 660-nm laser irradiation. Furthermore, the hybrid UCNPs also displayed an efficient PDT effect under the NIR laser light to a 3D model of MCF-7 tumor cell spheres, and could effectively inhibit the tumor growth through cellular DNA damage *in vivo*.

In addition to PAMAM dendrimers, other hydrophilic dendritic polymers have been explored to improve the water solubility of photosensitizers. For example, Luo et al. [45] employed 2,2-bis(hydroxymethyl) propionic acid (Bis-MPA) hyperbranched PEG-OH dendrimers to react with the photosensitizer of pyropheophorbide a (Ppa) to form a series of amphiphiles with different PEG molecular weights (20 and 10 kDa) and dendron generations (G2 and G3) for PDT of a mouse 4T1 tumor model. The amphiphile with 20 kDa PEG and G3 dendron showed the best tumor retention and antitumor PDT effect with a tumor growth inhibition reaching 96.0%. In another work, Luo and co-workers [46] also applied

glycopolymers with dendritic structures as vehicles to load PDT agents. They prepared a functionalized dendritic polymer conjugated with Ppa (denoted as DPP) for tumor metabolism interference-enhanced PDT of a 4T1 tumor model. In this work, the DPP was synthesized with a disulfide bond and a peptide linker integrating generation 3 glycodendron branches and Ppa, and could be broken up in the presence of glutathione and cathepsin B. *In vitro* results show that the DPP could effectively disturb 4T1 cellular metabolism, resulting in an increased energy depletion, dysfunctional H^+ regulation, as well as attenuated tolerance to oxidation stress. This led to augmented PDT *in vivo* with a much higher tumor inhibition efficiency (83.83%) than the control groups treated with only the linear Ppa-conjugated polymer counterpart (69.68%) or free Ppa (41.12%). Furthermore, the same group chemically conjugated the glycodendron and Ppa with hyaluronic acid for targeted drug delivery to CD44 receptor-expressing cancer cells [47]. The prepared nanosystem with a consolidated dendritic structure led to a much longer blood circulation and more accumulation at tumor sites than linear polymers, and significantly inhibited the growth of MDA-MB-231 tumor up to 99.2% in a mouse model under laser irradiation.

3.3. PTT

Dendrimer-based nanohybrids with an NIR absorption feature can be used for PTT of cancer cells *in vitro* and tumors *in vivo*. In an earlier study by Li et al., carboxylated G3.5 half-generation PAMAM dendrons were used as a stabilizer and reducing agent to prepare Au NPs with a size around 30 nm for photothermal ablation of HeLa cells (a human cervical carcinoma cell line) *in vitro*. The live-dead cell staining results demonstrated that the Au NPs prepared by DPG3.5-COOH had an obvious killing effect, while most of cells in the control group were still alive after laser irradiation [88]. To improve the biosafety profile and reduce the over-accumulation of Au NPs within the body, the Cheng group [64] was able to prepare dendrimer-stabilized Au NRs with a length of 10 nm and a higher PTT efficacy than that of Au DENPs for effective inhibition of PC-9 cells (non-small cell lung cancer cell line) *in vitro* and the xenografted tumor model *in vivo*. Similarly, Kono et al. [62] reported the use of PEG-PAMAM G3 dendrimers as a shell to stabilize the Au NR cores with excellent photothermal stability for effective PTT of HeLa cells *in vitro* and the xenografted mouse tumor model *in vivo* under an 808-nm laser irradiation. The tumor model treated with the GNR-cored PEG--PAMAM G3 dendrimers under laser irradiation exhibited a significant tumor suppression effect at 11 days post treatment.

In another work, Cui and coworkers [89] used RGD-conjugated dendrimer-modified Au NRs for targeted PTT of $\alpha_v\beta_3$ integrin-expressing tumors. The G4 PAMAM dendrimer was used to replace cetyltrimethylammonium bromide molecules on the surface of Au NRs to decrease their toxicity and improve their biocompatibility. With the RGD modification, the Au NRs exhibited targeting and devastating effects of A375 cancer cells (a human melanoma cell line) and xenografted A375 tumors under the laser irradiation. In a very similar work, the Cheng group [50] developed RGD-modified Pt DENPs with a Pt core size of 1.4 nm for PTT of xenografted MDA-MB-231 tumors overexpressing $\alpha_v\beta_3$ integrin. The authors showed that the targeted group exhibited much better therapeutic effect than the non-targeted one for tumor inhibition under the 808-nm laser irradiation.

In order to improve the tumor PTT efficacy, it is ideal to retain the Au NPs or Au NRs within the tumor region with relatively deep tumor penetration and long-time tumor retention. In a recent work, Cheng et al. [90] synthesized a degradable polymer hydrogel formed by crosslinking of aldehyde-modified dextran (Dex-Ald) with Pt DENPs *via* the imine bond formation. The hydrogel displayed a good photothermal conversion effect and biocompatibility, and was able to prolong the retention of therapeutic agents in tumors to achieve long-term and repeated PTT to eliminate tumors. *In vivo* assay showed that the hybrid hydrogel could allow repeated PTT to inhibit the tumor growth completely owing to the extended retention of the soft hydrogel in the tumors for more than one week.

In addition to the amine-terminated dendrimers described above that can be used for tumor treatment, dendrimers with different termini have also been exploited for cancer PTT. In a recent investigation, Cheng et al. [91] developed a multifunctional nanoplatform based on Pt DENPs templated by G5 PAMAM dendrimers with carboxyl termini (DEPt--COOH) for targeted PTT of malignant bone tumors. As a control material, amine-terminated Pt DENPs (DEPt-AC) were also synthesized to compare their tumor targeting specificity. *In vivo* biodistribution assay showed that the DEPt-COOH could be accumulated more in the osteolytic lesions around bone tumors than the DEPt-AC due to the targeting ability of high-density carboxyl groups on the surface of dendrimers that are sensitive to the hydroxyapatite crystals. In addition, *in vivo* antitumor results showed that the formed DEPt-COOH could inhibit bone tumors and osteolysis by PTT more effectively than the DEPt-AC.

3.4. Combination therapy

3.4.1. Combination PTT/chemotherapy

Phototherapy could be combined with other modalities of cancer therapy, such as chemotherapy, gene therapy, and radiotherapy (RT) etc., to improve the tumor treatment outcome. Mrówczyński and coworkers [92] developed a polydopamine-coated multifunctional nanocarrier consisting of PAMAM dendrimers of different generations and magnetite NPs (Fe_3O_4) and loaded with DOX to achieve cumulative effect of combination chemotherapy and PTT of liver cancer cells *in vitro*. In another work, Kono et al. [62] developed dendrimer-Au NR nanohybrids (PEG-DOX-PAMAM-Au NRs) with PEG-modified G4 PAMAM (PEG-PAMAM) as the shells and Au NRs as the core for combination PTT/chemotherapy of tumors. In their study, DOX was linked to the surface of PEG-PAMAM-Au NRs through pH-sensitive hydrazone bond with an acidic pH-triggered fast drug release profile, thus improving the chemotherapy outcome without side effects. *In vitro* and *in vivo* assays showed that the combination PTT and chemotherapy using the PEG-DOX-PAMAM-Au NRs exerted a significant synergistic therapeutic effect to mouse colon carcinoma 26 cancer cells and the xenografted tumor model by virtue of the acid-triggered DOX release and the excellent photothermal property of the Au NRs.

To realize PTT-regulated controllable and sustained drug release for enhanced combination tumor therapy, Wang et al. [93] recently developed an NIR light-responsive supramolecular hydrogel system composed of alpha-cyclodextrin (α-CD) and PEG-modified G5 PAMAM dendrimer-entrapped Pt NPs with photothermal property, and loaded an anticancer drug bortezomib (BTZ) within the hydrogel. The hybrid hydrogel could be degraded under laser irradiation to release the chemotherapeutics of BTZ, thereby realizing combination PTT/chemotherapy of PC-9 cancer cells *in vitro* under laser irradiation. In another work, the Ge group [94] synthesized a kind of thermal-responsive nanogels consisting of β-CD-modified G3 PAMAM dendrimers and adamantine (AD)-conjugated copolymer, poly [poly (ethylene glycol) monomethyl ether metharcylate]-co-poly (N-(2-hydroxypropyl)-methacrylamide)-co-poly (N-adamantan-1-yl-2-methacrylamide). The DOX and ICG could be encapsulated into the nanogels *via* electrostatic interaction. Under laser irradiation, the nanocomposites exhibited a light-triggered drug release, resulting in a significant decrease in the IC_{50} of DOX from 33 to 7 μg/mL, and were able to synergistically inhibit HepG2 cancer cells (a human hepatic cancer cell line) and xenografted H22 (a murine hepatic tumor) tumors through the combination PTT/chemotherapy.

3.4.2. Combination PDT/chemotherapy

To realize combination PDT/chemotherapy of tumors, Liu and coworkers [95] reported a novel light-responsive drug delivery platform for PDT/chemotherapy of 4T1 (a murine breast cancer cell line) tumors. In their design, Ce6-doped mesoporous silica NRs (CMSNRs) were used to load both the small molecular drug DOX and macromolecular drug G3-Pt

complexes, surface coated with bovine serum albumin (BSA) *via* a singlet oxygen–sensitive bis-(alkylthio) alkene (BATA) linker, and modified with PEG to produce CMSNR-BATA-BSA-PEG. The release of DOX or G3-Pt could be induced under the 660-nm laser irradiation due to the disconnection of BSA-PEG from the NR surface as controlled by the BATA linker breakup through singlet oxygen generated by Ce6. *In vitro* and *in vivo* assays showed that a remarkable synergistic therapeutic effect of combination PDT/chemotherapy could be realized.

To facilitate the deep tumor penetration of drug distribution, Zhou et al. [51] developed an NIR light–triggered dissociable liposomal nanoplatform by encapsulating cisplatin prodrug-grafted and ICG-loaded G5 PAMAM dendrimers within RGD-modified liposomes for light-assisted combination PDT/chemotherapy of deep tumors. In this work, ICG loaded within the dendrimer internal cavities could be released in a thermosensitive manner and small sized dendrimer/Pt prodrugs released could penetrate into the deep tumor tissues as triggered by laser irradiation. *In vivo* antitumor assay showed that the xenografted 4T1 tumors treated with the hybrid liposomes under laser irradiation possessed a high inhibition rate of 91.1% at 21 days after treatment, much higher than those in the other groups including single chemotherapy or single PDT.

3.4.3. Combination PDT/PTT

Dendrimer-based nanohybrids allow the incorporation of both PDT and PTT agents for combination PDT/PTT of tumors. In a recent work, Yuan et al. [66] reported the use of PAMAM-ICG complexes to construct a size-switchable polymeric NP (SNPICG/Ce6) for combination PDT/PTT of both normoxia and hypoxia regions of 4T1 tumors (Fig. 4). Through immunofluorescence images, the developed SNPICG/Ce6 complexes were demonstrated to be distributed into the deep tumor region under a 660-nm laser irradiation at 90 min after intravenous injection. The small-sized PAMAM-ICG was able to accumulate into the deep tumor tissues in hypoxic microenvironment for enhanced PTT of xenografted 4T1 tumors. Furthermore, owing to the photothermal effect of ICG, the size-switchable polymeric NPs displayed an excellent therapeutic effect under the laser irradiation for effective PTT of tumors. *In vivo* antitumor results showed that the therapeutic efficacy followed the order of PBS < SNP < SNP + 808 nm < SNP + 606 nm < inSNP + 606 nm + 808 nm < SNP + 606 nm + 808 nm. Overall, the developed SNPICG/Ce6 complexes with combination PPT/PDT therapy effect could inhibit tumor growth with an efficiency much higher than those of single PTT and PDT.

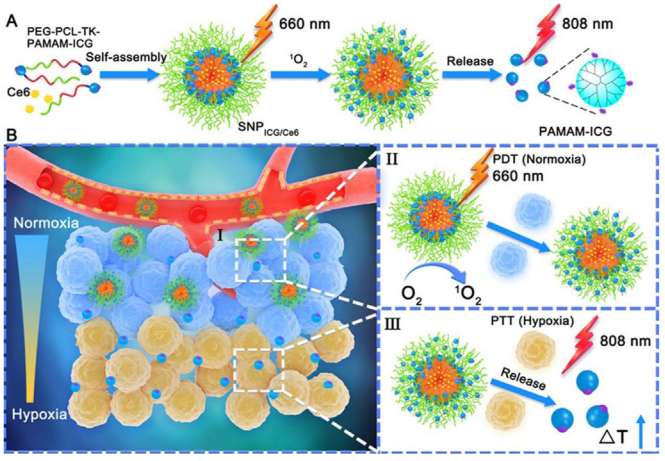

Fig. 4. (A) Schematic illustration of synthesis process of the PEG-b-PCL-TK-PAMAM-ICG *via* self-assembly of PEG-b-PCL and PAMAM-ICG linked with a singlet oxygen–responsive TK bond and singlet oxygen–mediated release of the small PAMAM-ICG from the SNPICG/Ce6 NPs. (B) The mechanism of PDT/PTT combination site-specific phototherapy. Reproduced with permission [66], Copyright 2020, American Chemical Society.

3.4.4. Other types of combination therapy

To combine gene therapy with PTT, our group designed G5-MoS_2/Bcl-2 siRNA nanohybrids [65]. With the excellent photothermal conversion efficiency and outstanding gene transfection efficiency in 4T1 cells to silence the Bcl-2 protein expression, the G5-MoS_2/Bcl-2 siRNA polyplexes could significantly improve the therapeutic efficacy of 4T1 cells *in vitro* and the subcutaneous tumor model *in vivo,* superior to single-modality PTT and gene therapy. For the same goal, Wu et al. [67] synthesized a pH-sensitive and charge-convertible nanocomplexes (GPCP/miR-21i/ICG) based on GO. Mouse TNBC tumor model treated with the GPCP/miR-21i/ICG nanocomplexes under laser irradiation exhibited a prominent tumor growth inhibition due to the miR-21i-based gene therapy and ICG-mediated phototherapy.

Tumor multidrug resistance is a major challenging issue in clinical tumor treatment. To solve this problem, Sun et al. [96] reported the modification of PAMAM dendrimers with a ligand containing ICG derivative cypate and iRGD peptide to load docetaxel (DTX) for chemo-phototherapy of HepG2 tumors. Under laser irradiation, the viability of DTX-resistant HepG2 cells treated with the target nanohybrids reached 6.62%, much lower than that treated with DTX-free functionalized dendrimers (11.51%) and free DTX (18.51%), displaying a synergistic effect of PTT/PDT/chemotherapy to overcome the multidrug resistance. *In vivo* antitumor assay also showed that the developed nanohybrids led to the best tumor inhibition and recurrence reduction under laser irradiation.

3.5. Theranostics

3.5.1. Fluorescence imaging-guided therapy

For highly efficient tumor diagnosis and therapy, it is crucial to integrate different imaging and therapeutic elements within one nanoplatform. In this context, dendrimers have played an important role in the development of different theranostic platforms for cancer nanomedicine. In an earlier study, Nava et al. [97] constructed a nanosystem by entrapment of Au NPs (diameter = 2.1 nm) within FA- and bombesin-grafted and ^{177}Lu-labeled G4 PAMAM dendrimers for fluorescence imaging due to the linked bombesin moieties, targeted RT due to the labeled radioisotope of ^{177}Lu and photothermal therapy owing to the entrapped Au NPs although the size of Au NPs is not optimal for PTT. In particular, the viability of T47D cancer cells (a human breast cancer cell line) significantly decreased after the cells were treated with the nanosystem along with laser irradiation and radiation of ^{177}Lu.

In another study, Taratula et al. [98] used G4 PPI dendrimers as a platform to encapsulate Pc within their internal cavities and to modify PEGylated LHRH peptide on their surface. The formed complexes exhibited a distinct NIR absorption (700 nm) and fluorescence emission (710 and 815 nm) features to facilitate PDT and fluorescence imaging. *In vitro and in vivo* imaging results revealed that the platform could be specifically internalized within the A2780/AD cancer cells (a human ovarian carcinoma cell line) and accumulated within the xenografted tumor model due to the LHRH-mediated targeting ability. In addition, the prepared formulation showed an excellent PDT effect with a low dark cytotoxicity (IC_{50} = 28 μg/mL) while excessive toxic reactive oxygen species generation could be triggered under light irradiation *in vitro*. Similarly, the same group [68] developed a multifunctional LOGr-Pc-PPI complex loaded with Pc as a photosensitizer to achieve NIR fluorescence imaging-guided combination PTT/PDT of a xenografted A2780/AD ovarian tumor model. Compared with the saline control group, the LOGr-Pc-PPIG4 group showed the stronger green fluorescence signal at 12 h after tail vein injection. In addition, the combination of PTT and PDT revealed a significant synergistic therapeutic effect with a high cell-killing efficiency of 90–95% against ovarian A2780/AD cancer cells at low Pc and LOGr dosages.

To realize fluorescence imaging-guided therapy through controlled drug release, Choi et al. [70] prepared a core-shell-type nanoplatform with the UCNPs as the cores and the shell composed of G5-FA dendrimers and

ONB-DOX complexes. The cellular uptake assay showed that KB cells (a human epithelial carcinoma cell line) with FA receptor overexpression had a more significant uptake of the platform than B16 cells (a mouse melanoma cell line) with low FA receptor expression, indicating the FA-mediated targeting specificity. Cell viability assay indicated that cells treated with the nanohybrids under the NIR and UV light irradiation had a lower viability than the dark control. These finding indicated that the developed core-shell nanohybrids could serve as a theranostic nanoplatform for a cell type–specific NIR fluorescence imaging and light-controlled drug release.

3.5.2. Photoacoustic (PA) imaging-guided therapy

Owing to the NIR absorption feature of the photoactive agents, dendrimer-based nanohybrids can be used for PA imaging-guided tumor therapy. To promote the deep tumor penetration for enhanced PTT/PDT/chemotherapy of tumors, Liu et al. [99] designed a dendrimer-based hybrid nanoplatform composed of biodegradable amphiphilic gelatin (AG) wrapped with doxorubicin and CuS-loaded arginine-conjugated G4 PAMAM dendrimers for PA imaging-guided deep tumor synergistic chemophototherapy (Fig. 5A). In this design, a dual cell-tissue penetration concept was proposed. First, the degradation of AG by metalloprotease can be accelerated under an 808-nm NIR laser irradiation to decompose the formed PRDCuS@AG nanocomposites with a size of 200–250 nm (PR represents arginine-conjugated PAMAM dendrimer) to form small arginine-rich PRDCuS NPs with a size of 7 nm. Second, with the arginine modification that is demonstrated to facilitate tumor cell membrane crossing, the PRDCuS NPs can lead to effective endocytosis and intercellular transportation into deep tumor tissues. The tumor penetration rate can be increased by 166.4% compared with control materials of PD@AG without PR (Fig. 5B). The PA imaging results showed that the signal value reached the maximum at 12 h after intravenous injection. *In vivo* antitumor results showed that the combined treatment of deep PTT/PDT and chemotherapy led to 97% of 4T1 tumor suppression efficiency, which is significantly better than the groups with other treatments. Interestingly, PRDCuS@AG can be eventually degraded into 3-nm ultra-small CuS NPs that can be effectively excreted from feces and urine to reduce their long-term toxicity.

To take the advantages of second NIR window (NIR-II, 1000-1700 nm) laser irradiation with greater tissue penetration depth, higher imaging signal-to-noise ratio and greater tissue tolerance than the first NIR (NIR-I, 650-950 nm) window laser irradiation, it is essential to develop dendrimer-based photomedicine incorporated with CuS NPs for PA imaging-guided tumor therapy. In a recent work, our group [61] developed RGD-CuS DENPs/pDNA nanocomplexes for targeted PA imaging-guided combination PTT/gene therapy of xenografted MDA-MB-231 tumors and inhibition of lung metastasis. Owing to the NIR-II absorption feature of CuS NPs and the RGD-mediated targeting specificity, the developed RGD-CuS DENPs/pDNA nanocomplexes enabled targeted PA imaging of $\alpha_v\beta_3$ integrin-expressing TNBC tumors. After intravenous injection of the RGD-CuS DENPs, the PA signal reached the maximum at 12 h after injection due to the long half-delay time (31.1 h) of the particles rendered by the zwitterionic surface modification of 1,3-PS. Meanwhile, owing to the zwitterionic surface modification–afforded antifouling property, the RGD-CuS DENPs/pDNA polyplexes enabled serum-enhanced gene transfection of HIC1-encoding pDNA *in vitro* and *in vivo* to efficiently inhibit cancer cell migration/invasion and lung metastasis, respectively. Furthermore, owing to the NIR-II absorption feature of the RGD-CuS DENPs/pDNA polyplexes, the particles displayed a favorable photothermal conversion efficiency (49.8%) under the NIR-II laser irradiation for effective PTT of tumors. Overall, the developed RGD-CuS DENPs/pDNA complexes enabled PA imaging-guided combination PTT/gene therapy to effectively inhibit tumor growth and tumor metastasis with an efficiency much higher than those of single PTT and gene therapy.

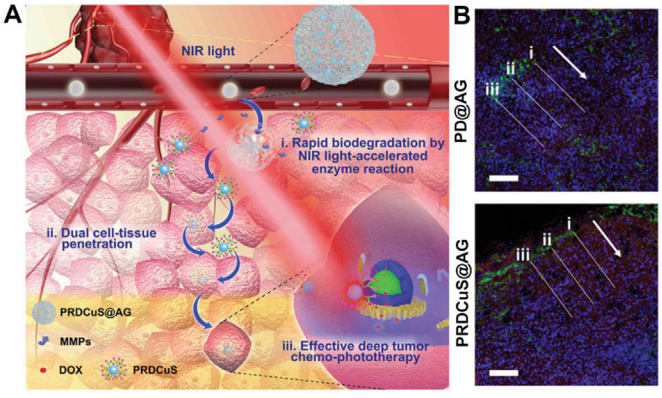

Fig. 5. (A) Schematic illustration of the PRDCuS@AG for deep tumor combination chemophototherapy. (B) 4T1 tumor section images after intravenous (i.v.) injection of PD@AG and PRDCuS@ AG (2 mg/mL, 100 μL) for 12 h. The corresponding fluorescence intensity of DAPI and DOX across along the lines in the 4T1 tumor section images are also shown. The arrow represents the direction of the lines. Blue (DAPI), nucleus; green (CD31), blood vessel; red, DOX. The concentration of DOX in PD@AG and PRDCuS@AG groups is equivalent. Scale bar is 100 μm. Reproduced with permission [99], Copyright 2020, Wiley-VCH.

3.5.3. Computed tomography (CT) imaging-guided therapy

For CT imaging-guided tumor therapy, our group [48] prepared dendrimer-assembled Au NSs modified with RGD peptide that were complexed with siRNA for combination PTT/gene therapy of tumors. Owing to the better X-ray attenuation property of Au NSs than that of Ominipaque, a conventional iodine-based CT contrast agent, the created nanohybrids can be used for CT imaging of tumors after intratumoral injection. The CT value increased 28.5 times higher at 10 min after intratumoral injection than preinjection. In addition, the surface amines of G3 PAMAM dendrimers render the nanohybrids with good gene compaction ability for efficient vascular endothelial growth factor (VEGF) siRNA delivery to silence the VEGF protein expression in the U87MG cancer cells (a human glioma cell line). Owing to the photothermal conversion efficiency (79%) and siRNA delivery ability of the RGD-Au DSNS/siRNA nanohybrids, *in vitro* cytotoxicity assay showed that the nanohybrids had a distinct killing effect to reduce the cell viability to 20.2% under laser irradiation, much lower than the other groups received single PTT or gene therapy. Likewise, *in vivo* assay data revealed that the developed RGD-Au DSNS/siRNA nanohybrids significantly suppressed the xenografted tumor model through the combination PTT/gene therapy with an efficiency much higher than those of the single PTT and gene therapy.

3.5.4. Dual-mode or multimode imaging-guided therapy

For precision cancer nanomedicine, it is essential to develop dual mode or multimode imaging techniques to guide tumor therapy. By virtue of the dendrimer nanotechnology, MR imaging can also be combined with NIR fluorescence imaging for dual-mode imaging-guided tumor therapy. For instance, Lin et al. [100] developed a core-shell structured nanocomposite for NIR fluorescence/MR imaging-guided PDT of tumors, where the UCNPs served as the core and the mitochondrial targeting molecule (3-carboxypropyl) triphenylphosphonium bromide–modified G4 PAMAM dendrimers with hydroxyl termini served as the shell. The involvement of the dendrimers enables the UCNPs to be water soluble, and makes it feasible to further load hydrophilic catalase (CTA) through electrostatic interaction, and meanwhile, the UCNPs with a hydrophobic layer could be loaded with hydrophobic photosensitizer Ce6 *via* hydrophobic interaction. The formed nanohybrids enabled mitochondrial targeting and depletion of hydrogen peroxide (H_2O_2) by CTA for oxygen generation to overcome tumor hypoxia for greatly enhanced PDT of a xenografted 4T1 tumor model.

Recently, our group [49] synthesized multifunctional Fe_3O_4/Au DSNFs for multimode CT/MR/PA imaging-guided combination PTT/RT of tumors (Fig. 6). The incorporated Au NFs and USIO NPs contributed

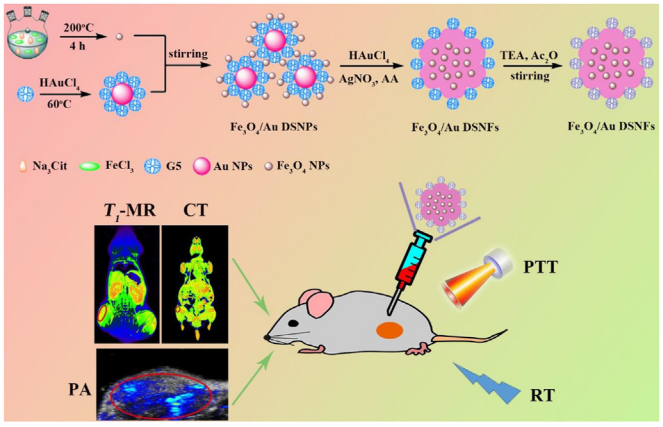

Fig. 6. The preparation and application of the Fe_3O_4/Au DSNFs for multimode imaging-guided combination PTT/RT of tumors. Reproduced with permission [49], Copyright 2018, Wiley-VCH.

CT/PA and MR imaging, respectively. Particularly, the designed Fe_3O_4/Au DSNFs had a much higher r_1 relaxivity (3.22 mM/s) than free USIO NPs due to the uniform distribution of USIO NPs within the Au NFs thanks to the role played by the dendrimer stabilizer and a higher photothermal conversion efficiency (82.7%) than pure Au NFs due to the doped high amount of USIO NPs within the Fe_3O_4/Au DSNFs that may play a synergistic reinforcing role by increasing the surface area of the Au NFs. At 60 min after intravenous injection of the Fe_3O_4/Au DSNFs, all the CT, MR, and PA signals reached the peak value simultaneously, demonstrating the imaging precision. Likewise, with the high photothermal conversion efficiency and excellent radiosensitization property of Fe_3O_4/Au DSNFs, the combination of PTT/RT could more significantly inhibit the growth of xenografted 4T1 tumors when compared with the single PTT and RT.

4. Conclusions and perspectives

In conclusion, owing to the well-defined structure and tunable surface activity of dendrimers, photosensitizer and photothermal agents could be integrated with dendrimers *via* covalent bonding, electrostatic interaction, or physical encapsulation or entrapment to form various organic/inorganic hybrid nanoconstructs including dendrimer-based metal and metal sulfide nanocomposites, dendrimer-based small molecular complexes, dendrimer-based carbon nanohybrids and dendrimer-based functional UCNPs. With the assistance of dendrimers, the generated nanohybrids display improved water dispersibility, colloidal stability, biocompatibility, imaging performance, or photothermal conversion efficiency. The current developed dendrimer-based nanohybrids with photomedicine components incorporated have been applied for different single or combination cancer treatment, as well as for different combinations of imaging-guided cancer therapy for precision cancer nanomedicine applications.

Despite the efforts that have been made so far to achieve numerous encouraging results related to dendrimer-based photomedicine for cancer imaging and therapy, there are still a range of challenges and rooms remaining unexplored. For instance, the inadequate accumulation of nanomaterials at tumor site and weak photoactivity of the nanohybrids deprive the efficiency of their phototherapy. Therefore, it is of necessity to further develop novel dendrimer-based phototherapeutics that are responsive to the specific features of tumor microenvironment, including for example slightly acidic pH and high levels of glutathione and reactive oxygen species to control the release and improve the penetration and aggregation of nanomaterials at tumor sites. In addition, dendrimers could serve as a platform to combine phototherapeutics with immune adjuvants or immune drugs, coordinating immunotherapy with phototherapy to magnify the antitumor efficacy and to inhibit tumor metastasis and recurrence. Furthermore, to improve the colloidal stability/biocompatibility and to prolong the blood circulation time of photomedicine, zwitterions could be modified onto the surface of dendrimers to render them with antifouling properties, although only one recent example from our group has been provided. Finally, ultrasound-targeted microbubble destruction and ionizing radiation techniques could be companied to improve the tumor accumulation and deep tumor penetration ability for improved treatment in deep lesions. From the aspect of clinical applications, it is apparent that the clinical translation of dendrimer-based hybrid photomedicines is still in its infancy. It is believed that exploring more possibilities to prepare various dendrimer-based hybrid photomedicines in GMP conditions and considering trials to examine in high-level animal models such as rat, rabbit, and pig, etc., will no-doubtfully help to boost the field of cancer nanomedicine and eventually facilitate smooth clinical translation.

Declaration of competing interest

The authors declare that they have no known competing financial interests or personal relationships that could have appeared to influence the work reported in this paper.

Acknowledgments

This research is financially supported by the National Key R&D Program (2017YFE0196200), the National Natural Science Foundation of China (81761148028 and 21773026), and the Science and Technology Commission of Shanghai Municipality (19410740200, 19XD1400100, and 20520710300).

References

[1] C.Y. Xing, S.Y. Chen, M. Qiu, X. Liang, Q. Liu, Q.S. Zou, Z.J. Li, Z.J. Xie, D. Wang, B.Q. Dong, L.L. Liu, D.Y. Fan, H. Zhang, Adv. Healthcare Mater. 7 (2018) 1701510.
[2] M. Qiu, W.X. Ren, T. Jeong, M. Won, G.Y. Park, D.K. Sang, L.P. Liu, H. Zhang, J.S. Kim, Chem. Soc. Rev. 47 (2018) 5588–5601.
[3] W. Tao, N. Kong, X. Ji, Y. Zhang, A. Sharma, J. Ouyang, B. Qi, J. Wang, N. Xie, C. Kang, H. Zhang, O.C. Farokhzad, J.S. Kim, Chem. Soc. Rev. 48 (2019) 2891–2912.
[4] Y.J. Liu, P. Bhattarai, Z.F. Dai, X.Y. Chen, Chem. Soc. Rev. 48 (2019) 2053–2108.
[5] L. Cheng, C. Wang, L.Z. Feng, K. Yang, Z. Liu, Chem. Rev. 114 (2014) 10869–10939.
[6] D.A. Tomalia, H. Baker, J. Dewald, M. Hall, G. Kallos, S. Martin, J. Roeck, J. Ryder, P. Smith, Polym. J. 17 (1985) 117–132.
[7] D.A. Tomalia, A.M. Naylor, W.A. Goddard, Angew. Chem. Int. Ed. 29 (1990) 138–175.
[8] B. Helms, E.W. Meijer, Science 313 (2006) 929–930.
[9] D.A. Tomalia, Prog. Polym. Sci. 30 (2005) 294–324.
[10] C.J. Hawker, J.M.J. Frechet, J. Am. Chem. Soc. 112 (1990) 7638–7647.
[11] Z.J. Xiong, M.W. Shen, X.Y. Shi, Sci. China Mater. 61 (2018) 1387–1403.
[12] C. Song, M.W. Shen, J. Rodrigues, S. Mignani, J.P. Majoral, X.Y. Shi, Coord. Chem. Rev. 421 (2020) 213463.
[13] Z.J. Xiong, C.S. Alves, J.H. Wang, A.J. Li, J.Y. Liu, M.W. Shen, J. Rodrigues, H. Tomas, X.Y. Shi, Acta Biomater. 99 (2019) 320–329.
[14] J. Qiu, L. Kong, X. Cao, A. Li, P. Wei, L. Wang, S. Mignani, A.M. Caminade, J.P. Majoral, X. Shi, Nanomaterials 8 (2018) 131.
[15] L.Z. Lin, Y. Fan, F. Gao, L.F. Jin, D. Li, W.J. Sun, F. Li, P. Qin, Q.S. Shi, X.Y. Shi, L.F. Du, Theranostics 8 (2018) 1923–1939.
[16] S.K. Choi, Chapter 10 - Photocontrolled nanosystems for antitumor drug delivery, in: S.k. Choi (Ed.), Photonanotechnology for Therapeutics and Imaging, Elsevier, 2020, pp. 277–2309.
[17] K. Tao, K. Sun, S.K. Choi, Chapter 12 - Upconversion nanocrystals for near-infrared-controlled drug delivery, in: S.k. Choi (Ed.), Photonanotechnology for Therapeutics and Imaging, Elsevier, 2020, pp. 345–371.
[18] J. Li, M.W. Shen, X.Y. Shi, ACS Appl. Bio Mater. 3 (2020) 5590–5605.
[19] C. Yang, Y. Gao, Y. Fan, L. Cao, J. Li, Y. Ge, W.Z. Tu, Y. Liu, X.Y. Cao, X.Y. Shi, Theranostics 11 (2021) 1721–1731.
[20] F. Chen, L.D. Kong, L. Wang, Y. Fan, M.W. Shen, X.Y. Shi, J. Mater. Chem. B 5 (2017) 8459–8466.
[21] C. Song, Y.C. Xiao, Z.J. Ouyang, M.W. Shen, X.Y. Shi, J. Mater. Chem. B 8 (2020) 2768–2774.
[22] X. Xue, J. Li, Y. Fan, M.W. shen, X.Y. Shi, Sci. China Mater. (2021), https://doi.org/10.1007/s40843-40020-41591-40841.
[23] C.Y. Liu, T. Wan, H. Wang, S. Zhang, Y. Ping, Y.Y. Cheng, Sci. Adv. 5 (2019), eaaw8922.
[24] H. Wang, W. Miao, F. Wang, Y.Y. Cheng, Biomacromolecules 19 (2018) 2194–2201.

[25] X.Y. Xu, K. Liu, Y. Wang, C.C. Zhang, M.H. Shi, P. Wang, L.H. Shen, J.D. Xia, L. Ye, X.Y. Shi, M.W. Shen, J. Mater. Chem. B 7 (2019) 3639–3643.
[26] J.Y. Liu, Z.J. Xiong, J.L. Zhang, C. Peng, B. Klajnert-Maculewicz, M.W. Shen, X.Y. Shi, ACS Appl. Mater. Interfaces 11 (2019) 15212–15221.
[27] Z. Qiao, X.Y. Shi, Prog. Polym. Sci. 44 (2015) 1–27.
[28] J.Y. Zhu, G.Y. Wang, C.S. Alves, H. Tomas, Z.J. Xiong, M.W. Shen, J. Rodrigues, X.Y. Shi, Langmuir 34 (2018) 12428–12435.
[29] Y. Xiao, X. Shi, Nanomedicine 14 (2019) 2515–2518.
[30] T.T. Xiao, J.B. Qin, C. Peng, R. Guo, X.W. Lu, X. Shi, Langmuir 36 (2020) 3096–3103.
[31] R.N. Liu, H.H. Guo, Z.J. Ouyang, Y. Fan, X.Y. Cao, J.D. Xia, X.Y. Shi, R. Guo, ACS Appl. Bio Mater. 4 (2021) 1803–1812.
[32] S.H. Wen, L.Z. Zhao, Q. Zhao, D. Li, C. Liu, Z. Yu, M.W. Shen, J.P. Majoral, S. Mignani, J.H. Zhao, X.Y. Shi, J. Mater. Chem. B 5 (2017) 3810–3815.
[33] X.Y. Xu, L.Z. Zhao, X. Li, P. Wang, J.H. Zhao, X.Y. Shi, M.W. Shen, Biomater. Sci. 5 (2017) 2393–2397.
[34] T.T. Xiao, D. Li, X.Y. Shi, M.W. Shen, Macromol. Biosci. 20 (2020) 1900282.
[35] L.Z. Zhao, J.Y. Zhu, Y.J. Cheng, Z.J. Xiong, Y.Q. Tang, L.L. Guo, X.Y. Shi, J.H. Zhao, ACS Appl. Mater. Interfaces 7 (2015) 19798–19808.
[36] X. Li, Z.J. Xiong, X.Y. Xu, Y. Luo, C. Peng, M.W. Shen, X.Y. Shi, ACS Appl. Mater. Interfaces 8 (2016) 19883–19891.
[37] S. Zamani, M. Shafeie-Ardestani, A. Bitarafan-Rajabi, A. Khalaj, O. Sabzevari, IET Nanobiotechnol. 14 (2020) 628–634.
[38] Y. Fan, W.Z. Tu, M.W. Shen, X.M. Chen, Y.S. Ning, J.J. Li, T.F. Chen, H. Wang, F.F. Yin, Y. Liu, X.Y. Shi, Adv. Funct. Mater. 30 (2020) 1909285.
[39] H.L. Cong, K.Q. Wang, Z.H. Zhou, J.J. Yang, Y. Piao, B. Yu, Y.Q. Shen, Z.X. Zhou, ACS Nano 14 (2020) 5887–5900.
[40] H. Cai, Y.F. Xiang, Y.J. Zeng, Z.Q. Li, X.L. Zheng, Q. Luo, H.Y. Zhu, Q.Y. Gong, Z.W. Gu, Y.H. Liu, H. Zhang, K. Luo, Acta Pharm. Sin. B 11 (2021) 544–559.
[41] Y. Fan, L.Z. Lin, F.F. Yin, Y. Zhu, M.W. Shen, H. Wang, L.F. Du, S. Mignani, J.P. Majoral, X.Y. Shi, Nano Today 33 (2020) 100899.
[42] J.Y. Zhu, L.Z. Zhao, Y.J. Cheng, Z.J. Xiong, Y.Q. Tang, M.W. Shen, J.H. Zhao, X.Y. Shi, Nanoscale 7 (2015) 18169–18178.
[43] Y. Fan, J. Zhang, M. Shi, D. Li, C. Lu, X. Cao, C. Peng, S. Mignani, J.P. Majoral, X. Shi, Nano Lett. 19 (2019) 1216–1226.
[44] J.Y. Zhu, L.F. Zheng, S.H. Wen, Y.Q. Tang, M.W. Shen, G.X. Zhang, X.Y. Shi, Biomaterials 35 (2014) 7635–7646.
[45] X.L. Zheng, D.Y. Pan, M. Chen, X.H. Dai, H. Cai, H. Zhang, Q.Y. Gong, Z.W. Gu, K. Luo, Adv. Mater. 31 (2019) 1901586.
[46] D.Y. Pan, X.L. Zheng, Q.F. Zhang, Z.Q. Li, Z.Y. Duan, W. Zheng, M. Gong, H.Y. Zhu, H. Zhang, Q.Y. Gong, Z.W. Gu, K. Luo, Adv. Mater. 32 (2020) 1907490.
[47] X.Q. Zhang, Y.H. Wu, Z.Q. Li, W.J. Wang, Y.P. Wu, D.Y. Pan, Z.W. Gu, R.L. Sheng, H. Tomas, H. Zhang, J. Rodrigues, Q.Y. Gong, K. Luo, Carbohydr. Polym. 247 (2020) 116749.
[48] P. Wei, J.W. Chen, Y. Hu, X. Li, H. Wang, M.W. Shen, X.Y. Shi, Adv. Healthcare Mater. 5 (2016) 3203–3213.
[49] S.Y. Lu, X. Li, J.L. Zhang, C. Peng, M.W. Shen, X.Y. Shi, Adv. Sci. 5 (2018) 1801612.
[50] Z.J. Zhou, Y.T. Wang, Y. Yan, Q. Zhang, Y.Y. Cheng, ACS Nano 10 (2016) 4863–4872.
[51] X. Xiong, Z. Xu, H.B. Huang, Y. Wang, J.Y. Zhao, X. Guo, S.B. Zhou, Biomaterials 245 (2020) 119840.
[52] P.M. Tiwari, K. Vig, V.A. Dennis, S.R. Singh, Nanomaterials 1 (2011) 31–63.
[53] N.S. Abadeer, C.J. Murphy, J. Phys. Chem. C 120 (2016) 4691–4716.
[54] B. Jang, J.Y. Park, C.H. Tung, I.H. Kim, Y. Choi, ACS Nano 5 (2011) 1086–1094.
[55] Y. Wei, R. Klajn, A.O. Pinchuk, B.A. Grzybowski, Small 4 (2008) 1635–1639.
[56] J. Huang, M. Guo, H.T. Ke, C. Zong, B. Ren, G. Liu, H. Shen, Y.F. Ma, X.Y. Wang, H.L. Zhang, Z.W. Deng, H.B. Chen, Z.J. Zhang, Adv. Mater. 27 (2015) 5049–5056.
[57] X. Li, L.X. Xing, K.L. Zheng, P. Wei, L.F. Du, M.W. Shen, X.Y. Shi, ACS Appl. Mater. Interfaces 9 (2017) 5817–5827.
[58] M. Zhou, R. Zhang, M. Huang, W. Lu, S.L. Song, M.P. Melancon, M. Tian, D. Liang, C. Li, J. Am. Chem. Soc. 132 (2010) 15351–15358.
[59] Q.W. Tian, F.N. Jiang, R.J. Zou, Q. Liu, Z.G. Chen, M.F. Zhu, S.P. Yang, J.L. Wang, J.H. Wang, J.Q. Hu, ACS Nano 5 (2011) 9761–9771.
[60] Y. Haba, C. Kojima, A. Harada, T. Ura, H. Horinaka, K. Kono, Langmuir 23 (2007) 5243–5246.
[61] Z.J. Ouyang, D. Li, Z.J. Xiong, C. Song, Y. Gao, R.N. Liu, M.W. Shen, X.Y. Shi, ACS Appl. Mater. Interfaces 13 (2021) 6069–6080.
[62] X. Li, K. Takeda, E. Yuba, A. Harada, K. Kono, J. Mater. Chem. B 2 (2014) 4167–4176.
[63] X. Li, M. Takashima, E. Yuba, A. Harada, K. Kono, Biomaterials 35 (2014) 6576–6584.
[64] X.Y. Wang, H.L. Wang, Y.T. Wang, X.T. Yu, S.J. Zhang, Q. Zhang, Y.Y. Cheng, Sci. Rep. 6 (2016) 22764.
[65] L.D. Kong, L.X. Xing, B.Q. Zhou, L.F. Du, X.Y. Shi, ACS Appl. Mater. Interfaces 9 (2017) 15995–16005.
[66] K.W. Wang, Y.L. Tu, W. Yao, Q.Y. Zong, X. Xiao, R.M. Yang, X.Q. Jiang, Y.Y. Yuan, ACS Appl. Mater. Interfaces 12 (2020) 6933–6943.
[67] C.H. Wu, Y. Tian, Y.X. Zhang, J.M. Xu, Y.K. Wang, X.T. Guan, T.T. Li, H. Yang, S. Li, X. Qin, Y.Y. Liu, Adv. Healthcare Mater. 9 (2020) 1901187.
[68] O. Taratula, M. Patel, C. Schumann, M.A. Naleway, A.J. Pang, H. He, O. Taratula, Int. J. Nanomed. 10 (2015) 2347–2362.
[69] B.Y. Wang, M.L. Liao, G.C. Hong, W.W. Chang, C.C. Chu, Nanomaterials 7 (2017) 269.
[70] P.T. Wong, D. Chen, S. Tang, S. Yanik, M. Payne, J. Mukherjee, A. Coulter, K. Tang, K. Tao, K. Sun, J.R. Baker Jr., S.K. Choi, Small 11 (2015) 6078–6090.
[71] M. Zhang, W.T. Wang, F. Wu, P. Yuan, C. Chi, N.L. Zhou, Carbon 123 (2017) 70–83.
[72] B.N. Eldridge, B.W. Bernish, C.D. Fahrenholtz, R. Singh, ACS Biomater. Sci. Eng. 2 (2016) 963–976.
[73] X.Y. Liang, W.T. Shang, C.W. Chi, C.T. Zeng, K. Wang, C.H. Fang, Q.S. Chen, H.Y. Liu, Y.F. Fan, J. Tian, Canc. Lett. 383 (2016) 243–249.
[74] J.T. Robinson, S.M. Tabakman, Y. Liang, H. Wang, H.S. Casalongue, D. Vinh, H. Dai, J. Am. Chem. Soc. 133 (2011) 6825–6831.
[75] K.P. Loh, Q. Bao, G. Eda, M. Chhowalla, Nat. Chem. 2 (2010) 1015–1024.
[76] G.M. Neelgund, A. Oki, Ind. Eng. Chem. Res. 57 (2018) 7826–7833.
[77] J.T. Robinson, K. Welsher, S.M. Tabakman, S.P. Sherlock, H. Wang, R. Luong, H. Dai, Nano research 3 (2010) 779–793.
[78] S. Han, T. Kwon, J.E. Um, S. Haam, W.J. Kim, Adv. Healthcare Mater. 5 (2016) 1147–1156.
[79] C.M. Hessel, V.P. Pattani, M. Rasch, M.G. Panthani, B. Koo, J.W. Tunnell, B.A. Korgel, Nano Lett. 11 (2011) 2560–2566.
[80] A. Punjabi, X. Wu, A. Tokatli-Apollon, M. El-Rifai, H. Lee, Y. Zhang, C. Wang, Z. Liu, E.M. Chan, C. Duan, G. Han, ACS Nano 8 (2014) 10621–10630.
[81] C.M. Andolina, P.J. Klemm, W.C. Floyd 3rd, J.M. Frechet, K.N. Raymond, Macromolecules 45 (2012) 8982–8990.
[82] C.C. Lee, E.R. Gillies, M.E. Fox, S.J. Guillaudeu, J.M. Frechet, E.E. Dy, F.C. Szoka, Proc. Natl. Acad. Sci. U. S. A. 103 (2006) 16649–16654.
[83] Q. Li, W. Gu, K. Liu, N. Xiao, J. Zhang, L.L. Shao, L. Li, S.T. Zhang, P. Li, RSC Adv. 6 (2016) 74560–74566.
[84] H.H. Yan, X.H. Gao, Y.F. Zhang, W.J. Chang, J.H. Li, X.W. Li, Q. Du, C. Li, ACS Appl. Mater. Interfaces 10 (2018) 17047–17057.
[85] K. Karki, J.R. Ewing, M.M. Ali, J. Nanomed. Nanotechnol. 7 (2016) 395.
[86] L. Zhang, N.R. Varma, Z.Z. Gang, J.R. Ewing, A.S. Arbab, M.M. Ali, J. Nanomed. Nanotechnol. 7 (2016) 404.
[87] Z.Y. Li, T.T. Lv, Y.Y. Zhang, L. Xu, L. Zhang, X.Y. Wang, H.J. Chen, Y. Gao, Dyes Pigments 154 (2018) 8–20.
[88] P. Dong, J.Y. Xin, X. Yang, J. Jia, W. Wu, J.S. Li, RSC Adv. 4 (2014) 44872–44878.
[89] Z.M. Li, P. Huang, X.J. Zhang, J. Lin, S. Yang, B. Liu, F. Gao, P. Xi, Q.S. Ren, D.X. Cui, Mol. Pharm. 7 (2010) 94–104.
[90] L. Li, C.P. Wang, Q. Huang, J.R. Xiao, Q. Zhang, Y.Y. Cheng, J. Mater. Chem. B 6 (2018) 2474–2480.
[91] Y. Yan, X. Gao, S. Zhang, Y.T. Wang, Z.J. Zhou, J.R. Xiao, Q. Zhang, Y.Y. Cheng, ACS Appl. Mater. Interfaces 11 (2019) 160–168.
[92] A. Jedrzak, B.F. Grzeskowiak, E. Coy, J. Wojnarowicz, K. Szutkowski, S. Jurga, T. Jesionowski, R. Mrowczynski, Colloids Surf., B 173 (2019) 698–708.
[93] X.Y. Wang, C.P. Wang, Q. Zhang, Y.Y. Cheng, Chem. Commun. 52 (2016) 978–981.
[94] M.H. Zan, J.J. Li, M.M. Huang, S.Q. Lin, D. Luo, S.Z. Luo, Z.S. Ge, Biomater. Sci. 3 (2015) 1147–1156.
[95] G.B. Yang, X.Q. Sun, J.J. Liu, L.Z. Feng, Z. Liu, Adv. Funct. Mater. 26 (2016) 4722–4732.
[96] R.F. Ge, J. Cao, J.N. Chi, S.C. Han, Y. Liang, L.S. Xu, M.T. Liang, Y. Sun, Int. J. Nanomed. 14 (2019) 4931–4947.
[97] H. Mendoza-Nava, G. Ferro-Flores, F.M. Ramirez, B. Ocampo-Garcia, C. Santos-Cuevas, E. Azorin-Vega, N. Jimenez-Mancilla, M. Luna-Gutierrez, K. Isaac-Olive, Mol. Imag. 2016 (2016) 1039258.
[98] O. Taratula, C. Schumann, M.A. Naleway, A.J. Pang, K.J. Chon, O. Taratula, Mol. Pharm. 10 (2013) 3946–3958.
[99] X.T. Pan, P.J. Li, L.T. Bai, J.J. Ma, S.S. Li, F.R. Zhang, S. Liu, Q.Y. Wu, H.Y. Shen, H.Y. Liu, Small 16 (2020) 2000809.
[100] S. Liang, C.Q. Sun, P.P. Yang, P.A. Ma, S.S. Huang, Z.Y. Cheng, X.F. Yu, J. Lin, Biomaterials 240 (2020) 119850.